Construction and Building Materials 141 (2017) 442–452

Contents lists available at ScienceDirect

Construction and Building Materials

journal homepage: www.elsevier.com/locate/conbuildmat

Investigation of rutting, fracture and thermal cracking behavior of asphalt mastic containing basalt and hydrated lime fillers

Aditya Kumar Das *, Dharamveer Singh

Civil Engineering Department, Indian Institute of Technology, Bombay 400076, India

HIGHLIGHTS

- Rutting performance and aging potential of asphalt mastic is greatly influenced by addition of hydrated lime filler.
- Combinations of basalt and hydrated lime fillers have significant influence on fracture properties of asphalt mastic.
- Hydrated lime with the combination of basalt filler exhibited good resistance to low temperature cracking of asphalt mastic.

ARTICLE INFO

Article history:
Received 28 December 2016
Received in revised form 28 February 2017
Accepted 5 March 2017

Keywords:
Hydrated lime (HL)
DENT
CTOD
Fracture
Creep stiffness
Rate of relaxation

ABSTRACT

The present study was undertaken to evaluate rutting, fracture and thermal cracking resistance behavior of asphalt mastic containing inert and active fillers. A control neat binder (AC-30) along with basalt (B) as an inert filler and hydrated lime (HL) as active filler were selected in this study. The asphalt mastics were prepared for different percentages of HL (5, 10, 15 and 20%) filler, in such a way that Filler to Binder (F/B) ratio becomes 0.8. A total of five combinations of asphalt mastic were prepared such as: AC-30 + 80% B + 0% HL, AC-30 + 75% B + 5%HL, AC-30 + 70% B + 10%HL, AC-30 + 65% B + 15%HL, and AC-30 + 60% B + 20% HL. The rutting, fracture and thermal cracking resistance of asphalt mastics was evaluated using Superpave rutting factor parameter, Double Edge Notched Tension (DENT) and Bending Beam Rheometer (BBR), respectively. Influence of HL on the performance of neat asphalt mastic was observed to be predominant in high-temperature range as obtained from the $G^*/Sin\delta$ value. The aging resistivity of asphalt mastic increased with the inclusion of HL, indicating a better rutting performance of asphalt mastic. The intermediate-temperature performance of asphalt mastic with HL was found to be higher compared to neat asphalt mastic from Critical Tip Opening Displacement (CTOD) results, implying better resistance to fracture. The addition of HL increased the low-temperature performance of asphalt mastic obtained from S(t) and m(t) values with S(t) and E(t) master curve, indicating enhanced resistance to thermal cracking. The combined effect of B and HL filler on the $G^*/Sin\delta$, CTOD, S(t), m(t) and E(t) parameters are presented in this study. In addition, ranking of asphalt mastics based on various parameters (i.e. CTOD and m(t)) is discussed in this paper.

1. Introduction

Asphalt mix consists of asphalt, aggregate, and mineral filler. The mixture of asphalt and mineral filler is usually called asphalt mastic. Mineral fillers are expected to contribute to the stability of asphalt mix by reducing voids and increasing stiffness [1,2]. Surface area, texture, type and elemental composition of mineral filler are major influencing factors affecting the performance of asphalt mastic [1,3]. Usually, inert and active fillers are used for the preparation of asphalt mastic. Stone dust, limestone, granite etc. are considered as inert filler, whereas, hydrated lime (HL), cement, fly ash, and diatomite etc. fall in the category of active filler. Active fillers like HL, diatomite are being used to improve antistripping and antiaging properties of asphalt mixes [4–6]. Numerous researchers showed that asphalt mix with active fillers showed enhanced rutting, fatigue and moisture damage resistance properties [4,7,8]. The filler to binder (F/B) ratio in the asphalt mix significantly affects the internal bonding between aggregates [9,10]. Tan Yi-qiu et al. [10] reported that asphalt mastic having F/B ratio within the range of 0.9–1.4 can have better mechanical performance.

Though inert fillers contribute to better rutting performance by increasing the stiffness of asphalt mix, they can make a mix

* Corresponding author.
E-mail addresses: kumaradityanitr@gmail.com (A.K. Das), dvsingh@iitb.ac.in (D. Singh).

http://dx.doi.org/10.1016/j.conbuildmat.2017.03.032
0950-0618/

Table 1
Basic physical properties of AC-30.

Test properties	Results	Standards
Penetration, 0.1 mm @ 25 °C	46	ASTM D5
Softening Point (°C)	48	ASTM D36
Ductility at 25 °C, mm	>100	ASTM D113
Absolute Viscosity @ 60 °C, Poise	Min. 2400	ASTM D2170

Table 2
Basic characteristics of fillers.

Fillers	SSA (m^2/g)	SG	HC
B	9.2	2.78	0.78
HL	11.3	2.2	0.81

*SSA (Specific surface area), SG (Specific gravity), HC (Hydrophilic coefficient).

susceptible to ductile failure and thermal cracking. Ductile failure/fracture of asphalt binder can happen at intermediate temperature. Recently developed Double Edge Notched Tension (DENT) is reported to be a reliable test to evaluate the ductile failure behavior of asphalt [11]. Thus, this test can also help in understanding cracking potential of asphalt mastic associated with yielding, ductility, and plasticity behavior by measuring specific work of failure and Critical Tip Opening Displacement (CTOD) values. A good correlation was reported between the CTOD value and fracture resistance of asphalt binder [12].

Similarly, low temperature thermal cracking in a flexible pavement occurs in cold regions. Due to rapid drop of temperature, thermal stresses develop in flexible pavement surface layer [13,14]. Bending Beam Rheometer (BBR) test is used to evaluate low temperature performance of asphalt binder and mastic based on stiffness and rate of relaxation properties [15]. Further, physicochemical interaction of binders and mineral fillers can influence the aging behavior of asphalt mastic. Aging commonly occurs due to oxidation and evaporation of volatile and light fractions of asphalt binder [16] and it can reduce elastic response of asphalt mastic, making it prone to cracking, especially at intermediate and low temperatures. Roman Lackner et al. [17] reported that low temperature creep stiffness of asphalt mastic was influenced because of random distribution of mineral filler particles within asphalt.

1.1. Research objectives

Few studies were reported to investigate combined effects of inert and active filler on the performance of asphalt mastic. The majority of the studies were concluded based on performance evaluation through Dynamic Shear Rheometer (DSR), and basic preliminary tests such as softening point, penetration, and viscosity. Hence, the present study was undertaken to evaluate intermediate temperature fracture failure and low temperature thermal cracking behavior of asphalt mastic with combinations of the inert and active fillers using DENT and BBR tests, respectively. Further, aging potential of fillers was evaluated by using Superpave rutting parameter with help of DSR test. Basalt (B) and hydrated lime (HL) were selected as an inert and active fillers, respectively. The proportion of HL was ranged from 0 to 20%. The F/B ratio was kept to 0.8. This ratio was selected as average value of standard range of 0.6–1.2 [18].

2. Materials and experimental program

2.1. Materials

A control asphalt binder (AC-30) was selected, which is commonly used for the construction of surface course of flexible pavements in India. The basic properties of AC-30 are given in Table 1. The B and HL were selected as inert and active fillers, respectively. Both fillers used for production of mastics in this research passed through the #200 sieve (75μ).

2.2. Characterization of fillers

The basic characterization of B and HL fillers was carried out using laser particle size and shape analyzer, BET-specific surface

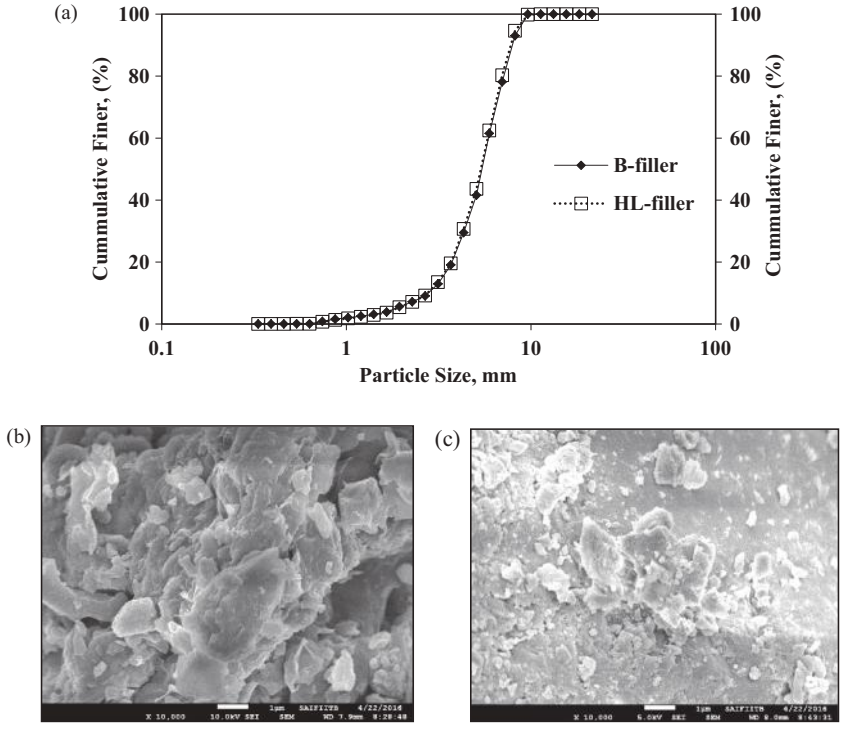

Fig. 1. (a) Particle size distribution curve of B and HL fillers; SEM imaging of (b) B filler and (c) HL filler, at a zoom level of 10,000 X.

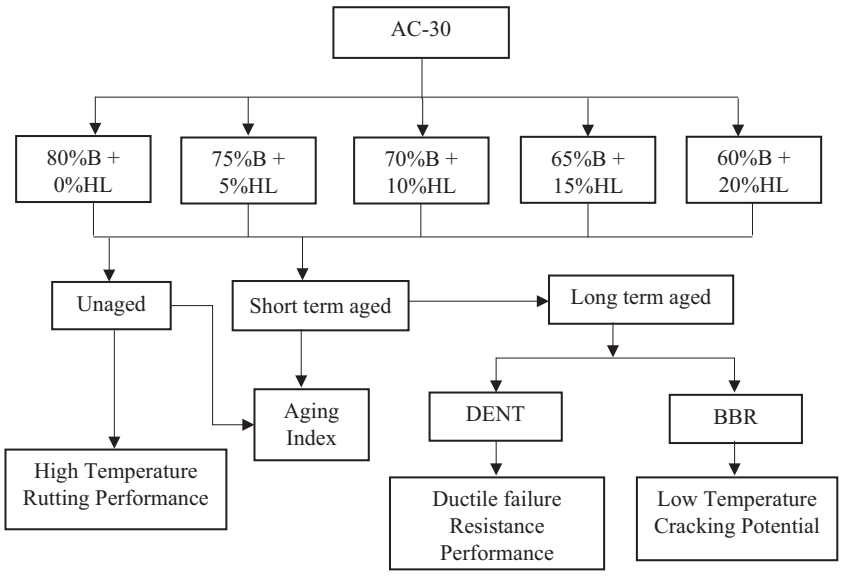

Fig. 2. Flow chart of the experimental program.

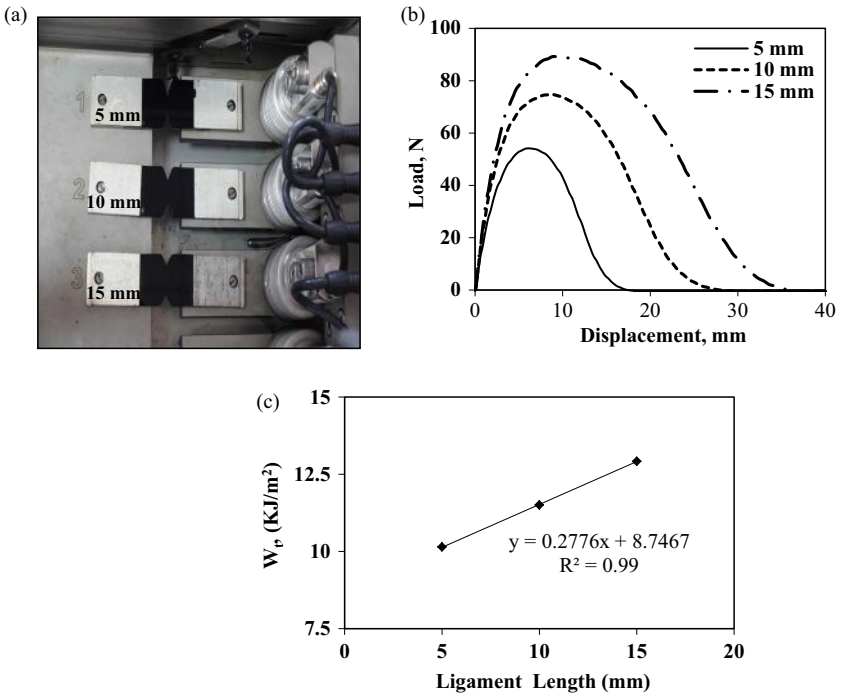

Fig. 3. (a) Typical DENT sample (b) load-displacement curve (c) TWF versus ligament length.

area (SSA) (Braunauer, Emmett, & Teller, 1938), specific gravity (SG), hydrophilic coefficient (HC) and scanning electron microscopy (SEM) imaging. The particle size distribution (Fig. 1) for both the fillers was found to be almost similar. The basic properties of B and HL fillers are given in Table 2.

The HC is a ratio of the volume of filler in water to the volume of filler in kerosene (JTG, E42). The HC determination is based on filler affinity to water [7]. If HC exceeds 1, then affinity of filler with water is more than that with asphalt. From the results, B filler showed less affinity to water than HL filler. SEM image of both the fillers is shown in Fig. 1. It can be seen that both the fillers are flaky in shape (Fig. 1).

2.3. Asphalt mastic preparation

Asphalt mastics (AC-30 mastic) were prepared by keeping F/B ratio of 0.8. Usually, 20% of HL by weight of asphalt binder is used in the preparation of asphalt mixes. The combination of filler (B and HL) was selected for preparation of asphalt mastic. The HL was varied from 0, 5, 10, 15 and 20% by weight of AC-30 binder, and B filler was adjusted accordingly to keep F/B = 0.8. Thus, five different combinations of asphalt mastic were prepared with B and HL fillers (i.e. (AC-30 + 80% B + 0% HL), (AC-30 + 75% B + 5% HL), (AC-30 + 70% B + 10% HL), (AC-30 + 65% B + 15% HL), and (AC-30 + 60% B + 20% HL)). To ensure moisture free surface, fillers

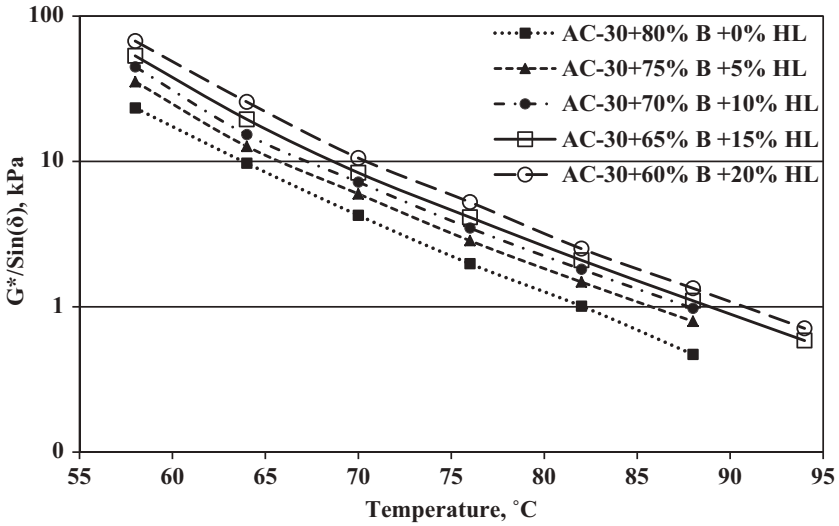

Fig. 4. Rutting factor ($G^*/Sin\delta$) versus temperature for different asphalt mastics.

were oven dried at 105 °C for 24 h. A 500 gm of AC-30 binder was preheated at 150 °C for 1 h in order to have proper fluidity for mixing it with fillers, taken for each combination of mastic samples. Oven dried fillers were added in hot AC-30 and mixed at 150 ± 5 °C using a mechanical mixer. The mixer was maintained at a stirring speed of 1500 r.p.m. for 1 h until formation of a homogeneous asphalt mastic.

2.4. Short Term and Long Term Aging

Short Term Aging (STA) was conducted to simulate loss of volatile components and oxidation of asphalt occurred in the field during mixing and compaction phase of asphalt mix layer. Long Term Aging (LTA) simulates progressive oxidation of asphalt mix occurred in the field [19]. The STA of asphalt mastics with all five combinations of B and HL fillers was done in the laboratory using thin film oven (TFO), conditioned for 5 h at 163 °C in accordance to ASTM D1754 [20]. Similarly, LTA of all asphalt mastic samples was done in the laboratory using pressure aging vessel (PAV) for 20 h by maintaining 2.1 MPa of air pressure at 100 °C. PAV aged residue was further conditioned for 30 min of degassing at 170 °C as per ASTM D 6521 [21]. The detail experimental program, implemented in this study is shown in Fig. 2.

3. Laboratory experimental plan

3.1. High failure temperature

The complex shear modulus (G^*) and phase angle (δ) of asphalt mastics for different combinations of B and HL fillers were measured at different temperature ranging from 58 to 94 °C (at 6 °C interval) using DSR using 25 mm parallel plate arrangement having 1 mm gap, subjected to loading frequency of 10 rad/s [22]. Thereafter, rutting factor ($G^*/Sin\delta$) was calculated for different types of asphalt mastics. The temperature corresponding to rutting factor value of 1 kPa (unaged) was considered as a failure temperature for respective asphalt mastic [23]. A higher value of $G^*/Sin\delta$ indicates better high-temperature performance of asphalt mastic.

3.2. Aging index (AI)

AI can explain aging resistivity of different types of asphalt mastics. AI was calculated for asphalt mastic with combinations of B and HL fillers based on unaged and short term aged rutting factor ($G^*/Sin\delta$) measured at 64 °C (considered being a maximum pavement temperature) using Eq. (1) [24]. A higher value of AI indicates a higher degree of aging susceptibility and vice versa.

$$\text{Aging Index (AI)} = \frac{(G^*/Sin\delta)_{aged}}{(G^*/Sin\delta)_{Unaged}} \quad (1)$$

3.3. Ductile failure potential using DENT test

The DENT test was used to evaluate effects of fillers on ductile failure behavior of asphalt mastic at an intermediate temperature. The DENT test was carried out on PAV aged asphalt mastic with all five combinations of B and HL fillers at 25 °C. The test was conducted for 5 mm, 10 mm and 15 mm ligament lengths (Fig. 3(a)) at a strain rate of 100 ± 2.5 mm/min using a force ductilometer testing machine in accordance with AASHTO TP 113 [25]. Two replicates were taken for each sample and the average values are reported. The DENT test results in total specific work of fracture (TWF), essential work of fracture (EWF), non-essential or plastic work of failure (NEWF) and CTOD. The TWF was calculated from the force-displacement curve (Fig. 3(b)) using Eq. (2). The TWF is the sum of essential and non-essential or plastic work of failure as shown in Eq. (2).

$$W_t = \int_0^{t_f} P \times \mathrm{d} = W_e + W_p \quad (2)$$

where W_t is TWF in kJ/m^2; w_e is EWF in kJ/m^2; w_p is NEWF in MJ/m^3; t_f is the time when ductile failure reached; P is the tensile load applied in N and d is the respective displacement in mm. Eq. (2) can be rewritten as follows:

$$W_t = W_e + W_p = LB \times w_e + \beta L^2 B \times w_p \quad (3)$$

A plot between w_t and ligament length, L mm, (Fig. 3(c)) was used to estimate w_e and w_p. The intercept and slope of the best fit straight line indicate w_e and plastic work (βw_p), respectively. Specific total work of failure (w_t) was calculated using Eq. (4)

$$w_t = W_t/LB = w_e + \beta w_p L \quad (4)$$

The CTOD value is a well-known parameter to indicate ductile failure and strain tolerance behavior of asphalt [26]. The CTOD value is inversely proportional to the amount of distress or cracking [27]. The CTOD value was calculated for the smallest ligament length of 5 mm using Eqs. (5 & 5(a)).

Table 3
Failure temperature and aging index of asphalt mastics for different asphalt mastics.

Asphalt mastics	failure temperature (°C)		G*/Sin(δ), kPa @64 °C		
	Unaged	Short term aged	Unaged	Short term aged	Aging index
AC-30 + 80% B + 0% HL	82	89	9.72	24.5	2.52
AC-30 + 75% B + 5% HL	86	90	12.7	31.5	2.48
AC-30 + 70% B + 10% HL	88	92	15.3	36.3	2.37
AC-30 + 65% B + 15% HL	89	93	19.5	40.8	2.09
AC-30 + 60% B + 20% HL	91	96	25.7	47.5	1.85

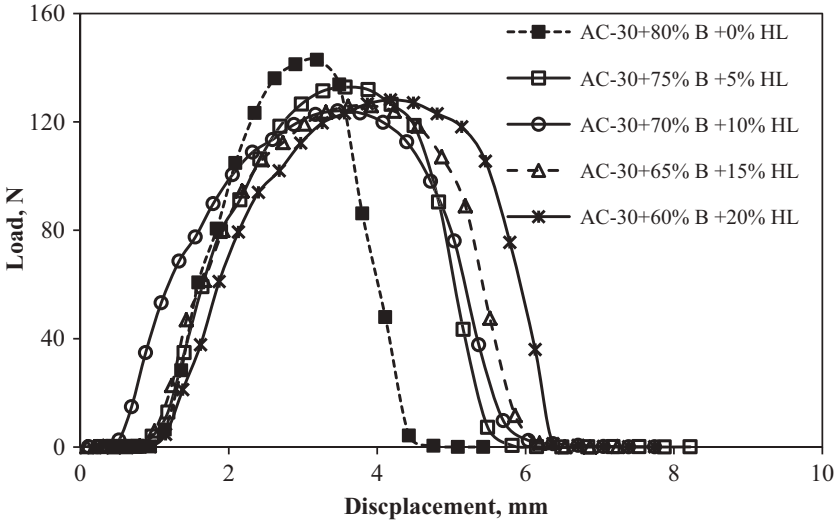

Fig. 5. Load versus displacement curve for 5 mm ligament length.

Table 4
Peak load and failure deformation for all five asphalt mastics.

Mastics	Peak load, N	Failure deformation, mm
AC-30 + 80% B + 0% HL	143	4.34
AC-30 + 75% B + 5% HL	133	4.9
AC-30 + 70% B + 10% HL	131.8	5.1
AC-30 + 65% B + 15% HL	129.4	5.8
AC-30 + 60% B + 20% HL	128	6.46

$$CTOD_{(5\ \mathrm{mm})} = \frac{w_e}{\sigma_n} \tag{5}$$

$$\sigma_{n,(5\ \mathrm{mm})} = \frac{P_{peak}}{BL} \tag{5a}$$

where σ_n is net section stress, N/mm^2, P_{peak} is average maximum load, N.

3.4. Low temperature cracking resistance using BBR test

3.4.1. Creep stiffness and rate of relaxation

Creep stiffness (S(t)) and rate of relaxation (m(t)) of five different asphalt mastics were measured using BBR test as per ASTM D 6648. The influence of HL on the thermal cracking potential of the asphalt mastic was investigated at five different temperatures of 0, −3, −6, −9 and −12 °C. The low temperature performance was carried out on different asphalt mastic beam samples, subjected to a constant load of 100 g (980 ± 50 mN) for 240 s. The S(t) can be calculated using Eq. (6).

$$S(t, 60\ \mathrm{s}) = \frac{PL^3}{4bh^3\delta(t)} \tag{6}$$

where P is constant load applied, N; δ(t) is a time-dependent deflection of the beam at mid-span; L is the beam length, mm; b width of the beam; and h is the thickness of the beam. The S(t) values were evaluated for 8, 15, 30, 60, 120 and 240 s of time. The slope at 60 s of the plot between logarithmic of S(t) with logarithmic of time, is reported as the m(t) value. The m(t) value was calculated using Eq. (6(a)).

$$m(t, 60\ \mathrm{s}) = \left|\frac{dLogS(t = 60\ \mathrm{s})}{dLogt(60\ \mathrm{s})}\right| \tag{6a}$$

Analysis of the influence of HL on the low temperature thermal cracking performance of asphalt mastic was based on limiting values of 'S(t) (<300 MPa)' and 'm(t) (>0.3)' as per ASTM D6816.

3.4.2. Master curve

Master curve of S(t) and relaxation modulus (E(t)) was obtained for five different asphalt mastics. The master curves were obtained to investigate trend of S(t) & E(t) over time domain based on the rate of increase or decrease of the slope to reach the glassy state (3000 MPa). The S(t) and E(t) master curves were generated using Christensen-Anderson Marasteanu (CAM) model (Eq. (7)) as per ASTM D6816 at a reference temperature of −6 °C. The S(t) was replaced with E(t) for generating E(t) master curve.

$$S(T_{ref}, \xi) = S_{glassy}\left[1 + \left(\frac{\xi}{\lambda}\right)^{\beta}\right]^{-kappa/\beta} \tag{7}$$

where S (T_{ref}, ξ) = Stiffness at reduced time in MPa, 'ξ'; S_{glassy} = Glassy modulus assumed as 3 GPa; λ, β and k are shape parameters. The E(t) of AC-30 mastics was calculated from measured S(t) data using Power-Law-Based inter-conversion procedures proposed by

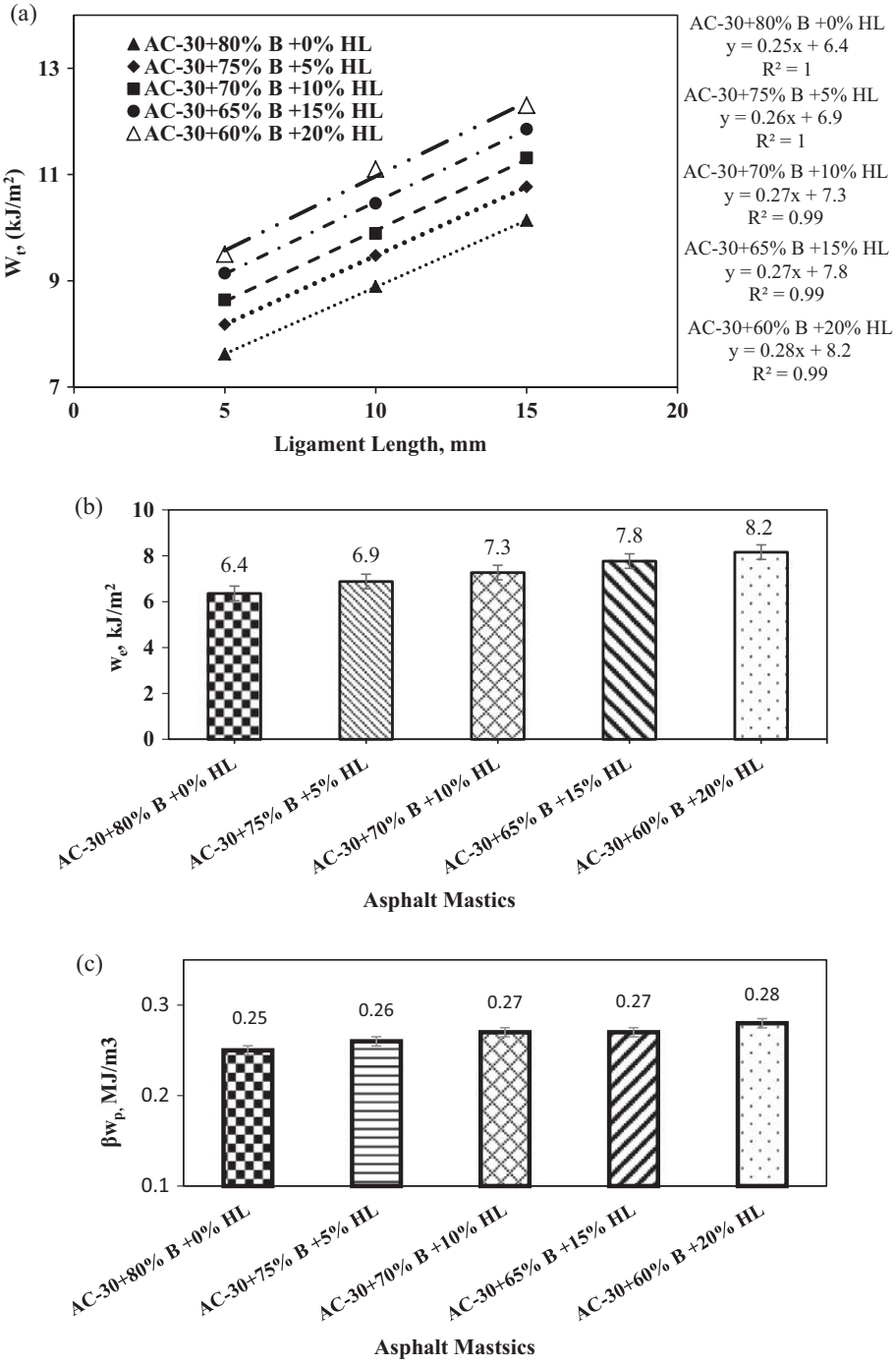

Fig. 6. (a) Total specific work of fracture versus ligament length; (b) specific essential work for AC-30 mastics with HL filler; (c) specific non-essential work for AC-30 mastics with HL filler.

Leaderman (1958) [28]. Creep Compliance (D(t)) of asphalt can be derived from S(t) using Eq. (8).

$$D(t) = 1/S(t) \tag{8}$$

$$E(t)D(t) = \frac{Sin(n\pi)}{(n\pi)} \tag{9}$$

$$n = \left|\frac{dLogF(\tau)}{dLog\tau}\right|_{at\ \tau=t} \tag{9a}$$

where F(τ) is source function of either D(τ) or E(τ), n is a function of t. E(t) is relaxation modulus in MPa, D(t) is creep compliance in MPa^{-1}.

4. Results and discussions

4.1. High failure temperature

Superpave rutting parameter value ($G^*/Sin\delta$) of unaged asphalt mastics with 0, 5, 10, 15 and 20% HL is shown in Fig. 4. The results

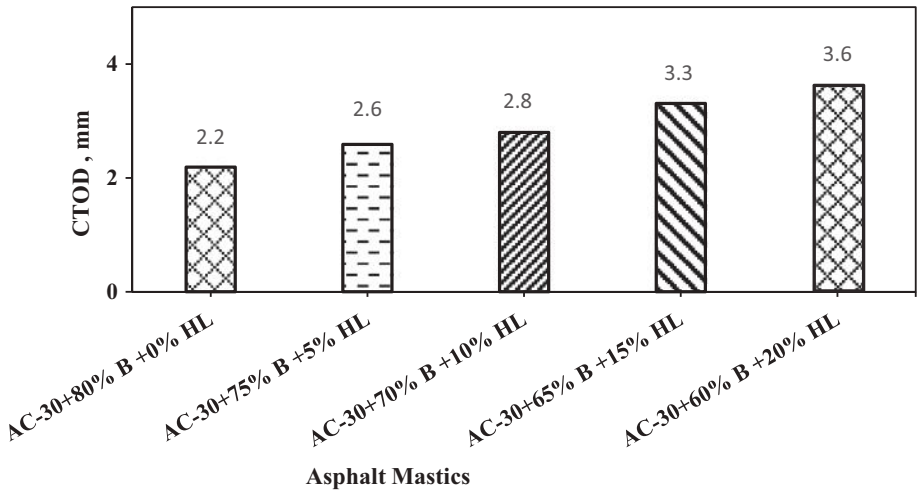

Fig. 7. CTOD values for AC-30 mastics with different percentage of HL.

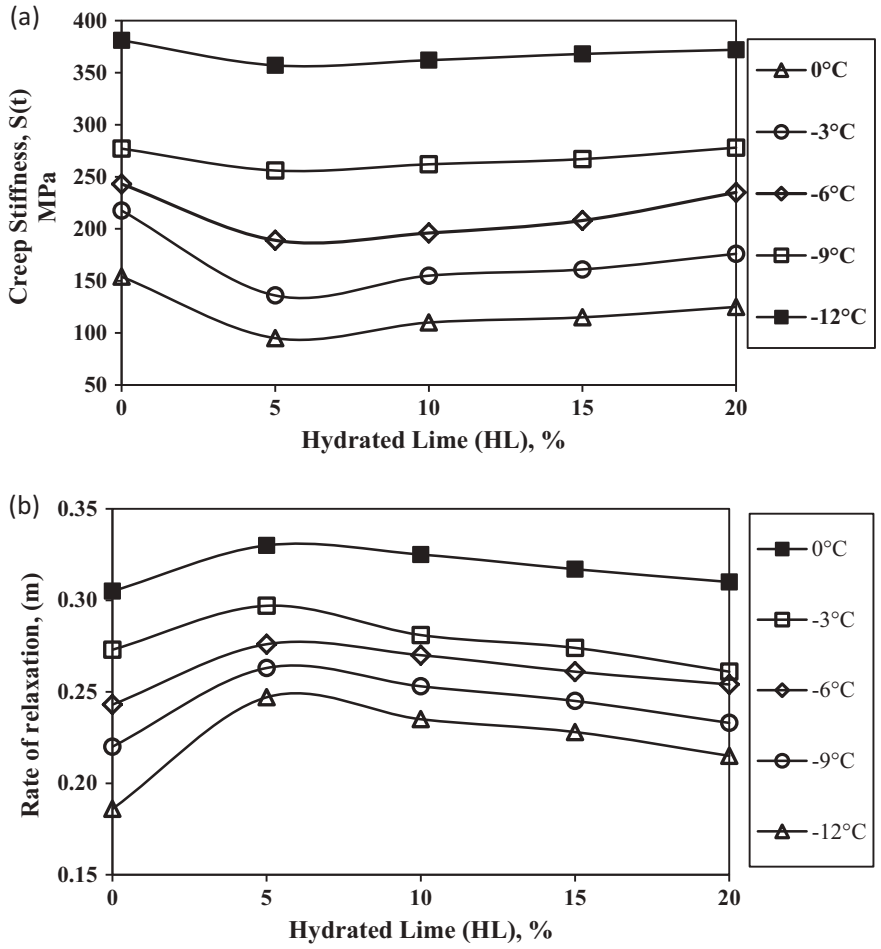

Fig. 8. (a) Creep stiffness value for AC-30 mastic with different HL content (b) 'm'- value for AC-30 mastic with different HL content.

shown in Fig. 4 indicate that G*/Sinδ value increases with an increase in HL percentage. Asphalt mastic with the addition of 5% HL shows a prominent increase in G*/Sinδ value, which can be considered as a significant improvement in rut resistance. Further addition of HL from 10% to 20% showed a marginal improvement in G*/Sinδ value. Moreover, failure temperature of asphalt mastic with 0, 5, 10, 15 and 20% HL was found to be 82, 86, 88, 89 and 91 °C, respectively (Table 3). It is evident that failure temperature increased with an increase in HL content. Also, an increase in G*/Sinδ by an amount of 25–63% was observed with every failure temperature improvement of asphalt mastic for all combinations of B & HL filler. Hence, it can be concluded that addition of HL

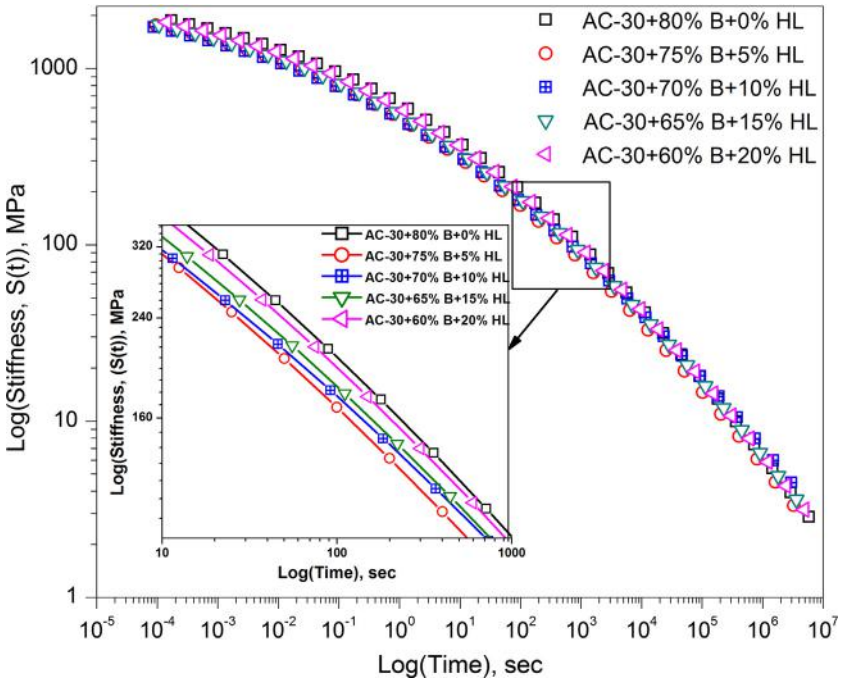

Fig. 9. Creep stiffness master curve for different asphalt mastic at −6 °C.

enhanced rutting resistance of asphalt mastic, which may be attributed to agglomeration tendency of HL particles in asphalt mastic structure [2].

4.2. Aging index

The AI value for asphalt mastics with 0, 5, 10, 15 and 20% HL was found to be 2.52, 2.48, 2.37, 2.09 and 1.85, respectively at 64 °C (Table 3). The results show that the AI value decreases with increase in HL percentage, indicating enhanced aging resistance of asphalt mastic with the addition of HL. The HL performs as an antioxidant agent in asphalt mastic phase which affects the binder response to aging, and consequently its molecular distribution, thus resulting in reduced AI value [2,16].

4.3. Cracking potential using DENT test

4.3.1. Influence of HL on load versus displacement curve

Fig. 5 shows a load-displacement curve for different combinations of asphalt mastics. The peak in the curve corresponds to the yielding of asphalt mastic around the ligament area. Deformation at failure for asphalt mastic with 0, 5, 10, 15 and 20% HL was found to be 4.34, 4.9, 5.1, 5.8 and 6.46 mm, respectively (Table 4). Also, peak load for asphalt mastics with 0, 5, 10, 15 and 20% HL was found to be 143, 133, 131.8, 129.4 and 128 N, respectively. The curves for neat asphalt mastic (0% HL) showed a noticeable load drop over the peak point (Fig. 5) and thus, exhibited the lowest deformation at failure with the highest peak load, indicating its brittle nature (Table 4). However, an increase in deformation at failure and decrease in peak load were observed with an increase in HL percentage (Table 4). Moreover, HL showed a notable improvement in the load-displacement curve, which is clear indication of a change in the behavior of asphalt mastic from brittle to ductile transition phase.

4.3.2. Influence of HL on work of fracture

Fig. 6(a) shows the plot of TWF values obtained from load-displacement data using Eq. (2). Fig. 6(a) shows that an increase in HL from 0% to 20% HL resulted in an increase in TWF (at 5 mm ligament length) value from 7.6 kJ/m^2 to 9.5 kJ/m^2. Increase in TWF with addition of HL improved the yielding capacity (with improved fracture energy) of asphalt mastic. A similar trend can also be observed at other ligament lengths. Thus, it can be concluded that HL plays a prominent role in enhancing fracture energy of asphalt mastic.

The intercept and slope of the line indicate w_e and w_p, respectively. Asphalt binder with a relatively high value of 'w_e' is considered to have good resistance to ductile failure [29]. Fig. 6(b) represents the variation of w_e values with different percentage of HL. It can be observed that w_e of asphalt mastic with 0% HL (6.4 kJ/m^2) increased to 8.2 kJ/m^2 with addition of 20% HL (Fig. 6 (b)). Thus, increase in w_e with addition of HL shows better fracture behavior of asphalt mastic.

Fig. 6(c) shows the variation of w_e values with different percentage of HL. This comparison shows marginal changes in the plastic behavior of asphalt mastic with the addition of HL. Thus, HL exhibited a positive role by enhancing plastic behavior of asphalt mastic (Fig. 6(c)). A binder with a high value of 'w_p' can possess good resistance to fatigue cracking [30].

4.3.3. Influence of HL on CTOD value

The variation of CTOD value with 0, 5, 10, 15 and 20% HL was calculated using Eq. (5) and shown in Fig. 7. The CTOD value of asphalt mastic with 0, 5, 10, 15 and 20% HL was found to be 2.2, 2.6, 2.8, 3.3 and 3.6 mm, respectively. It can be seen that the CTOD value of asphalt mastic increased with the addition of HL (Fig. 7), indicating better resistance to fracture (enhanced resistance to ductile failure). The increase in CTOD values is not very substantial with an increase in HL. However, addition of higher percentage of HL (20%) increased CTOD by 50%, implying a better resistance to fracture. It is expected that antiaging property of HL might have attributed to an increase in CTOD of asphalt mastic., Based on the CTOD value, the ductile failure or fracture resistance of different types of asphalt mastics can be ranked as (AC-30 + 60% B + 20% HL) > (AC-30 + 65% B + 15% HL) > (AC-30 + 70% B + 10% HL) > (AC-30 + 75% B + 5% HL) > (AC-30 + 80% B + 0% HL).

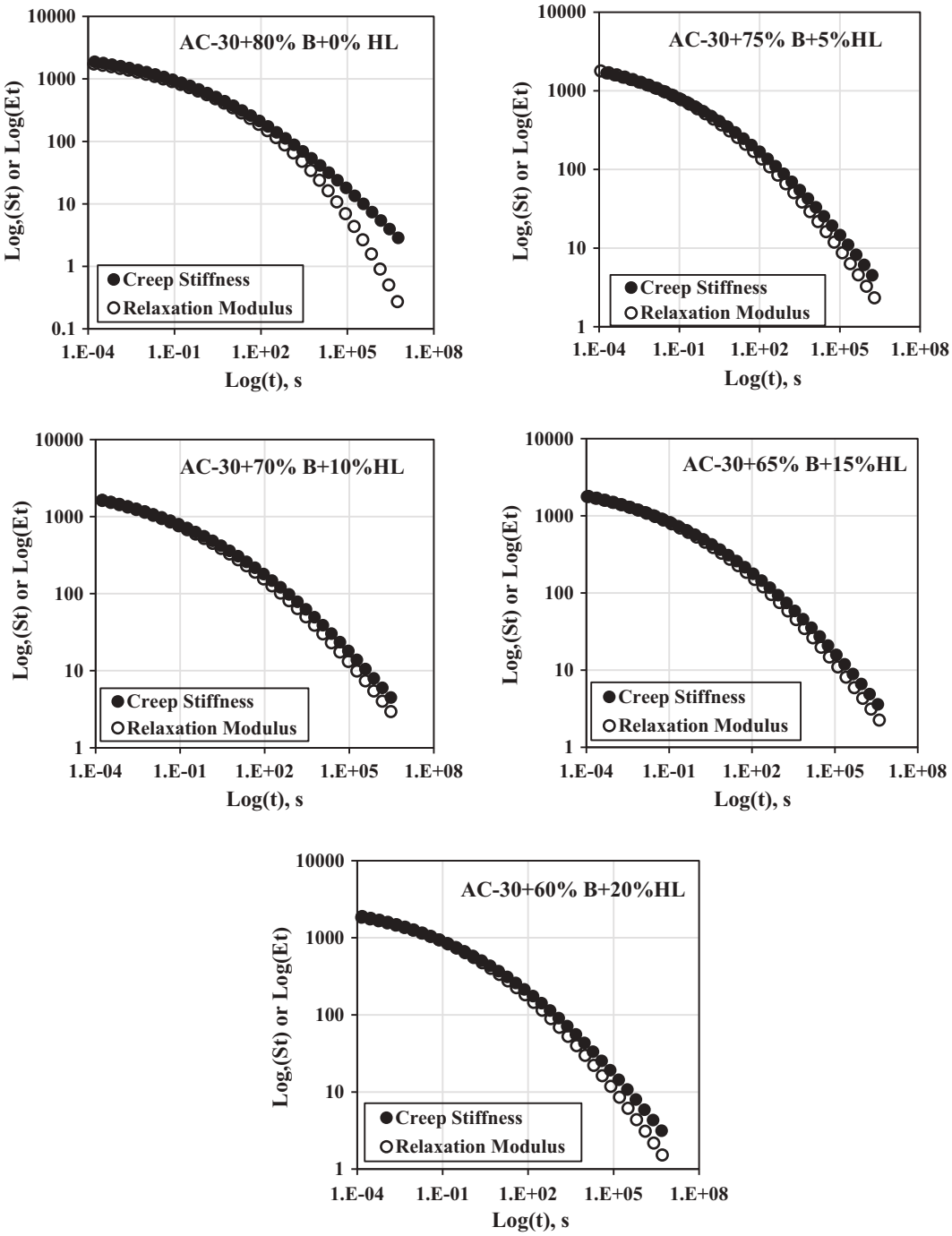

Fig. 10. Relaxation modulus master curve for different asphalt mastics at −6 °C.

4.4. Low-Temperature fracture resistance using BBR TEST

4.4.1. Influence of HL on creep stiffness and rate of relaxation

Fig. 8(a) represents variations in S(t) value (at 60 s) with 0, 5, 10, 15 and 20% HL at 0, −3, −6, −9 and −12 °C. A lower value of S(t) (<300 MPa) is desired for an asphalt binder to have a good resistance to low temperature thermal cracking [13,30]. The S(t) value for asphalt mastic containing 0, 5, 10, 15 and 20% of HL was found to be 243, 189, 196, 208 and 235 MPa, respectively at −6 °C. The S (t) of asphalt mastic with addition of HL showed lower value compared to neat asphalt mastic, indicating improvement in thermal cracking resistance. The curve of Fig. 8(a) shows that a decrease in S(t) value of asphalt mastic until addition of 5% HL and a slight increase with further addition of HL by 10, 15, 20% at −6 °C. This may be because of decrease in low temperature hardening of asphalt mastic with the addition of HL and thus, decrease in stiffness property [2,16]. Similar behavior of S(t) curve can also be observed at 0 °C, −3 °C, −9 °C and −12 °C. However, asphalt mastic containing 0, 5, 10, 15 and 20% HL showed S(t) values of 381, 358, 362, 368 and 372 MPa, respectively at −12 °C. These resulting high values of S(t) (>300 MPa) indicating lesser resistance to thermal cracking. This may be attributed to the substantial increase in S (t) value beyond −9 °C. Hence, it can be concluded that HL plays an influencing role to enhance the low-temperature performance of neat asphalt mastic up to a temperature of −9 °C.

Similarly, m(t)-value was measured at 0, −3, −6, −9 and −12 °C to understand the effect of HL on the stress relaxation behavior of asphalt mastic. A higher m(t)-value (>0.3), indicates the slower

development of thermal stress [31]. The m(t)-value of asphalt mastic with 0, 5, 10, 15 and 20% HL was measured to be 0.243, 0.280, 0.272, 0.261 and 0.252 respectively, at −6 °C (Fig. 8(b)). Also, the m(t)-value of asphalt mastic with 0, 5, 10, 15 and 20% HL was found to be 0.305, 0.330, 0.325, 0.317 and 0.310, respectively at 0 °C.

It can be seen that addition of 5% HL increases m(t) value of asphalt mastic, indicating an increase in stress relaxation ability. However, further addition of HL by 10–20% showed (Fig. 8(b)) a slight decrease in m(t) value, but higher value as compared to neat asphalt mastic. Similar trend in the m(t) curve of asphalt mastics was resulted at 0 °C, −3 °C, −9 °C and −12 °C. Further, asphalt mastic with 0%–20% HL showed a low value of m(t) (<0.3) at −6 °C, indicating lesser resistance to thermal cracking. However, at 0 °C asphalt mastic with 0%–20% HL exhibited comparative high values of m(t) (>0.3), which can be considered as enhanced resistance to thermal cracking. Based on m(t), thermal cracking resistance of different asphalt mastics can be ranked as: (AC-30 + 75% F + 5% HL) > (AC-30 + 70% F + 10% HL) > (AC-30 + 65% F + 15% HL) > (AC-30 + 60% F + 20% HL) > (AC-30 + 80% F + 0% HL).

4.4.2. Creep stiffness and relaxation modulus master curves

The S(t) master curve for asphalt mastic with 0, 5, 10, 15 and 20% HL at −6 °C is shown in Fig. 9. It can be seen that asphalt mastic with HL shows reduced stiffness values compared with the neat asphalt mastic (0% HL). Asphalt mastic with 5% HL showed a comparatively faster decrease in slope followed by asphalt mastic with 10%, 15%, 20% and 0% HL (Fig. 9).

Also, it can be observed that addition of HL exhibited lesser S(t) value for all loading time range, indicating a slower increase in slope to reach the glassy state (S(t) = 3000 MPa). This slower increase in slope implies the slower development of thermal stress, which can result in improved resistance to thermal cracking. Hence, it can be concluded that HL has a tendency to improve low-temperature performance, which may be due to the inclusion of HL filler particles inside asphalt mastic.

E(t) is an essential parameter for calculation of thermal stress. The thermal stress progression is directly related to the development of relaxation modulus. Therefore, S(t) and m(t) values must play an important role in the development of thermal stress [32]. Fig. 10 represents E(t) versus reduced time for different asphalt mastics estimated using Eq. (9). It can be observed that S(t) and E(t) are identical in nature and their slope is close to zero on a double logarithmic scale for a very short period of time. The rate of decrease in E(t) is faster than S(t) value with increase in time, indicating a decrease in the rate of thermal stress development.

From Fig. 10, it can also be noted that the rate of decrease in E(t) is comparatively little faster than S(t) with decrease in loading time and this trend of the slope is similar for all combination of asphalt mastics with HL (0%–20%). Further, asphalt mastic with 5% HL showed a faster rate of decrease in E(t) followed by asphalt mastic prepared with 10%, 15%, 20%, and 0% HL, which can be considered as a comparative increase in ability to resist thermal stress development.

5. Conclusions

The present study focused on rutting, fracture and low temperature cracking potential of asphalt mastic containing basalt and hydrated lime as inert and active fillers, respectively. The following critical conclusions can be drawn based on the results and discussion presented above:

a. Addition of hydrated lime as an active filler increased rutting resistance and decreased aging potential of asphalt mastic.
b. The load carrying capacity increased and deformation at failure decreased with addition of HL, indicating improved ductile nature of asphalt mastic.
c. The CTOD value of asphalt mastic increased with an increase amount of HL. The asphalt mastic with 20% HL (60% B + 20% HL) was found to be superior followed by 15%, 10%, 5% and 0% HL.
d. Addition of HL decreased creep stiffness and increased m-value of asphalt mastic. Further, asphalt mastic with HL showed decreased slope of S(t) and E(t) for all range of loading time. The asphalt mastic with 5% HL (75% B + 5% HL) was found to have better low-temperature thermal cracking performance.

References

[1] F.P. Jimenez, R.M. Recasens, A. Martinez, Effect of filler nature and content on the behavior of bituminous mastics, RMPD 9 (sup1) (2008) 417–431.
[2] V. Antunes, A.C. Freire, L.R. Quaresma, R. Micaelo, Influence of the geometrical and physical properties of filler in the filler–bitumen interaction, Constr. Build. Mater. 76 (2015) 322–329.
[3] S.C. Huang, M. Zeng, Characterization of aging effect on rheological properties of asphalt-filler systems, Int. J. Pavement Eng. 8 (3) (2007) 213–223.
[4] D.N. Little, J.C. Petersen, Unique effects of hydrated lime filler on the performance-related properties of asphalt cements: physical and chemical interactions revisited, J. Mater. Civ. Eng. 17 (2) (2005) 207–218.
[5] M. Iwanski, G. Mazurek, Hydrated lime as the anti-aging bitumen agent, Proc. Eng. 57 (2013) 424–432.
[6] Y. Cheng, J. Tao, Y. Jiao, Q. Guo, C. Li, Influence of diatomite and mineral powder on thermal oxidative ageing properties of asphalt, Adv. Mater. Sci. Eng. 2015 (2015) 1–10.
[7] Y. Cheng, J. Tao, Y. Jiao, G. Tan, Q. Guo, S. Wang, P. Ni, Influence of the properties of filler on high and medium temperature performances of asphalt mastic, Constr. Build. Mater. 118 (2016) 268–275.
[8] J. Wu, G. Airey, The influence of mineral fillers on mastic aging properties, in: Proceedings, ICCTP 2011, ASCE, Nanjing, China, 2011, pp. 3450–3061.
[9] H. Qiu, X. Tan, S. Shi, H. Zhang, Influence of filler–bitumen ratio on performance of modified asphalt mortar by additive, J. Mod. Transp. 21 (1) (2013) 40–46.
[10] T. Yi-qiu, Z.H. Li, X.Y. Zhang, Z.J. Dong, Research on high-and low-temperature properties of asphalt-mineral filler mastic, J. Mater. Civ. Eng. 22 (8) (2010) 811–819.
[11] A. Andriescu, S. Hesp, J. Youtcheff, Essential and plastic works of ductile fracture in asphalt binders, Transp. Res. Rec.: J. Transp. Res. Board 2004 (1875) 1–7.
[12] N. Gibson, X. Qi, A. Shenoy, G. Al-Khateeb, M.E. Kutay, A. Andriescu, Full-scale accelerated performance testing for superpave and structural validation, Final Rep. FHWA-RT-01946, Federal Highway Administration, Washington, DC, 2011.
[13] M. O. Marasteanu, R. Velasquez, A. Zofka, A. Cannone Falchetto, Development of a simple test to determine the low temperature creep compliance of asphalt mixtures, Transportation Research Board (TRB), Washington, DC, NCHRP IDEA Rep. 133, 2009.
[14] K.H. Moon, M.O. Marasteanu, M. Turos, Comparison of thermal stresses calculated from asphalt binder and asphalt mixture creep tests, J. Mater. Civ. Eng. 25 (8) (2013) 1059–1067.
[15] H.U. Bahia, D.A. Anderson, D.W. Christensen, The bending beam rheometer; a simple device for measuring low-temperature rheology of asphalt binders (with discussion), J. AAPT 61 (1992).
[16] Shin-Che Huang, J. Claine Petersen, Raymond E. Robertson, Jan F. Branthaver, Effect of hydrated lime on long-term oxidative aging characteristics of asphalt, Transp. Res. Rec.: J. Transp. Res. Board 2002 (1810) 17–24.
[17] R. Lackner, M. Spiegl, R. Blab, J. Eberhardsteiner, Is low-temperature creep of asphalt mastic independent of filler shape and mineralogy?—arguments from multiscale analysis, J. Mater. Civ. Eng. 17 (5) (2005) 485–491.
[18] MoRTH, 5th Revision, Specifications for road and bridgeworks, Ministry of Road Transport and Highways Indian Roads Congress, New Delhi, India, 2013.
[19] R. Liang, S. Lee, Short-term and long-term aging behavior of rubber modified asphalt paving mixture, Transp. Res. Rec.: J. Transp. Res. Board 1530 (1996) 11–17.
[20] ASTM: D 1754, Standard Test Method for Effects of Heat and Air on Asphaltic Materials (Thin-Film Oven Test), American Society for Testing and Material, 2014, pp. 1–6.
[21] ASTM: D 6521, Standard Practice for Accelerated Aging of Asphalt Binder Using a Pressurized Aging Vessel (PAV), American Society for Testing and Material, 2013, pp. 1–6.
[22] ASTM: D 7175, Standard Test Method for Determining the Rheological Properties of Asphalt Binder Using a Dynamic Shear Rheometer (DSR), American Society for Testing and Material, 2005, pp. 1–16.
[23] A. Behl, S. Chandra, V.K. Aggarwal, S. Gangopadhyay, Zero shear viscosity of bitumen-filler mastics of warm-mix binders, J. Mater. Civ. Eng. 27 (10) (2014) 1–6.
[24] P.K. Ashish, D. Singh, S. Bohm, Investigation on influence of nanoclay addition on rheological performance of asphalt binder, RMPD (2016) 1–20.

[25] AASHTO: TP 113, Standard method of test for Determination for Asphalt Binder Resistance to Ductile Failure Using Double Edge Notched Tension (DENT) Test, AASHTO International, 2015, pp. 1–9.
[26] A. Andriescu, N. Gibson, S. Hesp, X. Qi, J. Youtcheff, Validation of the essential work of fracture approach to fatigue grading of asphalt binders, J. AAPT 75 (2006) CD1.
[27] M. Paliukaite, M. Verigin, S.A.M. Hesp, Double-edge-notched tension testing of asphalt cement for the control of cracking in flexible asphalt pavements, Bituminous Mixtures Pavements VI 13 (2015).
[28] S.W. Park, Y.R. Kim, Interconversion between relaxation modulus and creep compliance for viscoelastic solids, J. Mater. Civ. Eng. 11 (1) (1999) 76–82.
[29] H.K. Agbovi, Effects of low temperatures, repetitive stresses and chemical aging on thermal and fatigue cracking in asphalt cement pavements on highway 417 (MSc thesis), Department of Chemistry, Queen's University, Kingston, Canada, 201).
[30] O.P. Togunde, Low temperature investigations on asphalt binder performance – a case study on highway 417 trial sections (MSc thesis), Department of Chemistry, Queen's University, Kingston, Canada, 2008.
[31] D. Sowah-Kuma, Assessment of low temperature cracking in asphalt pavement mixes and rheological performance of asphalt binders (MSc thesis), Department of Chemistry, Queen's University, Kingston, Canada, 2015.
[32] M. Marasteanu, Role of bending beam rheometer parameters in thermal stress calculations, Transp. Res. Rec.: J. Transp. Res. Board 2004 (1875) 9–13.